DNA methylation alterations of *PITX2* and *PANCR* are associated with left-right asymmetry of the heart and left ventricle size

Steffan Noe Niikanoff Christiansen[1,2], Kristine Boisen Olsen[3], Sara Tangmose Larsen[3], Pernille Heimdal Holm[3], Marie Kroman Palsøe[3], Marie-Louise Kampmann[1], Stine Bøttcher Jacobsen[1], Mikkel Meyer Andersen[4], Jytte Banner[3], Niels Morling[1], Jacob Tfelt-Hansen[1,5], Jeppe Dyrberg Andersen[1]

[1] Section of Forensic Genetics, Department of Forensic Medicine, Faculty of Health and Medical Sciences, University of Copenhagen

[2] Department of Health Science and Technology, The Faculty of Medicine, Aalborg University, Denmark

[3] Section of Forensic Pathology, Department of Forensic Medicine, Faculty of Health and Medical Sciences, University of Copenhagen

[4] Department of Mathematical Sciences, Aalborg University

[5] The Department of Cardiology, The Heart Centre, Copenhagen University Hospital, Rigshospitalet, Copenhagen, Denmark

1 Abstract

Background

Postmortem genetic testing is a crucial tool to determine the cause of sudden cardiac death and to allow family testing of relatives. While DNA variants are extensively studied in sudden cardiac death, the role of DNA methylation alterations is poorly understood. In contrast to DNA variants, DNA methylation is tissue-specific. Therefore, it is essential to determine the most relevant anatomical regions for tissue sampling. We aimed to assess the importance of standardised sampling procedures in the investigation of DNA methylation in the human ventricles.

Methods and results

We used the Infinium MethylationEPIC array technology to profile the DNA methylation levels among 771,458 CpG sites in the left ventricle, septum, and right ventricle of 15 individuals who died due to sudden cardiac death. We identified 256 differentially methylated regions in the left and right ventricles and the septum. Notably, regions differentially methylated in the left and right ventricles were located in proximity to genes overrepresented in gene ontology terms related to the formation and growth of the human heart. Furthermore, the left ventricle size was correlated with DNA methylation alterations in proximity to the *PITX2* (Pearson's R^2 = 0.54, P = 0.007) and *PANCR* genes (Pearson's R^2 = 0.51, P = 0.009). We observed no clustering among the samples from the left and right ventricles and the septum. The top 0.1% most variable sites (n = 771) clustered by individual rather than by anatomical origin.

Conclusion

We showed that DNA methylation alterations near *PITX2* and *PANCR* are associated with left-right asymmetry and left ventricle size. Furthermore, our findings highlight the importance of standardised tissue collection from multiple regions of the cardiac ventricles in postmortem DNA methylation investigations of the human heart.

2 Introduction

Sudden cardiac death (SCD) accounts for hundreds of thousands of deaths in Europe every year (Jean-Philippe et al. 2022). In 45% of the cases, SCD is the first manifestation of a cardiovascular disease (Skjelbred et al. 2025), thereby highlighting the urgent need for diagnostic tools capable of identifying individuals at risk. Potentially inherited cardiac diseases, including different cardiomyopathies and primary arrhythmogenic disorders, are estimated to account for 43-78% of the SCDs in individuals aged 1-49 years, and in up to 54% of the cases, the cause of death remains unexplained even after autopsy (Lynge et al. 2022).

Postmortem genetic testing identified pathogenic or likely pathogenic genetic variants in 13% of sudden arrhythmic death syndrome (SADS) cases (Lahrouchi et al. 2017) and in 18% of SCDs with structural alterations of the heart (Lahrouchi et al. 2020). A significant advantage of postmortem genetic testing is the ability to uncover arrhythmogenic disorders that may not be detected through standard autopsy procedures. Furthermore, postmortem genetic testing enables cascade screening of family members. Consequently, postmortem genetics testing is recommended in unexplained SCDs (Stiles et al. 2021; Wilde et al. 2022; Zeppenfeld et al. 2022).

While DNA variants have been extensively studied in postmortem investigations, other molecular alterations that may influence the risk of SCD remain poorly understood. One such alteration, DNA methylation, has been widely studied in the context of cardiac disease (Haas et al. 2013; Grunert et al. 2016; Meder et al. 2017; Pepin et al. 2019a, 2019b; Sutter et al. 2024; Chen et al. 2025) However, its role in SCD has not been well explored. DNA methylation, which involves the addition of a methyl group to cytosines in CpG dinucleotides, is generally associated with reduced gene expression in promoter regions (Schultz et al. 2015; Gilsbach et al. 2018) . Despite extensive investigations of the role of DNA methylation in cardiac diseases, the level of DNA methylation heterogeneity of the human heart is mainly unknown, potentially introducing bias in studies where cardiac tissues are collected from different anatomical locations. To examine how tissue sampling of different anatomical locations of the ventricles may influence DNA methylation investigations, we profiled the methylome of the left ventricle (LV), the septum (S), and the right ventricle (RV).

We showed that tissue sampling of different anatomical locations in the ventricles influences DNA methylation investigations. Furthermore, we identified differentially methylated regions (DMRs) among LV, S, and RV located near genes associated with the growth and formation of the chambers of the heart. Last, we showed that the DMRs between LV and S are correlated with the volume of the left ventricle.

3 Materials and Methods

3.1 Design of the study

The heart tissue samples were collected from autopsies of 15 individuals in 2018 at the Section of Forensic Pathology, Department of Forensic Medicine, University of Copenhagen. All deaths were categorised as SCDs. The tissue samples were collected from the mid-ventricular sections of the hearts as part of the standard examination of the heart, as recommended by the Association for European Cardiovascular Pathology (Basso et al. 2017). LV and RV samples were collected from the anterior wall of the ventricles. The samples were only included if they showed no or little decomposition, since high levels of decomposition of cardiac tissues alter the DNA methylation levels (Poggiali et al. 2024). The samples were stored at -70 °C before DNA was extracted for further analyses.

3.2 DNA methylation array investigations

DNA from frozen tissue was extracted using the DNeasy Blood & Tissue Kit (Qiagen, Germany) following the manufacturer's recommendations. The DNA was prepared for methylation measurements with an input amount of 200 ng (Christiansen et al. 2022). The resulting sodium bisulfite-treated DNA was examined using the Infinium MethylationEPIC v2.0 Kit (Illumina, USA) that detects the methylation levels of more than 930,000 positions using a probe-based approach.

3.3 Data analysis

The data analysis was performed in the statistical environment R (version 4.3.1) using the *tidyverse* (version 2.0.0) (Wickham 2014; Wickham et al. 2019) and *patchwork* (version 1.2.0) (Pedersen 2024) packages.

The SeSAMe package (v1.20.0) was used to convert the raw intensity (.idat) data files into normalised methylation values using the *openSesame* function with the default preprocessing code ("QCDPB") (Zhou et al. 2018). In brief, the preprocessing steps include masking poorly designed probes ("Q"), inferring channels for Infinium I probes ("C"), performing non-linear dye bias correction ("D"), removing probes with high out-of-band (OOB) signals ("P"), and conducting background subtraction using out-of-band signals ("B"). The probes were annotated with the "EPICv2.hg38.manifest.gencode.v41.tsv" annotation file obtained from https://github.com/zhou-lab/InfiniumAnnotation (Kaur et al. 2023). Only data from chromosomes 1-22 were included in the analyses.

Methylation levels from array experiments were reported as either β-values or M-values (Supplementary Methods 1). In brief, the β-values were calculated as the ratios of methylated signal compared to the total signal (reported as a value between 0 and 1). The M-values were reported as values between -Infinity and Infinity. The

M-values were preferred for analyses because the variance is approximately constant (Du et al. 2010). To address unwanted batch variation in the normalised methylation values, the *ComBat()* function from the *sva* package (Leek et al. 2012) was used (Supplementary Methods 2). The adjusted M-values were used for the principal component analysis (PCA) and the exploration of the most variable positions. The PCA was conducted using the base R *prcomp* function in R with centred and scaled values. The four components explaining the largest fraction of variability were visualised. Heat maps were visualised with the *pheatmap* package (v.1.0.12) with the Euclidean distance as a similarity measure and complete linkage for clustering.

Pearson's correlation coefficient was calculated to estimate the correlation among the samples. The squared correlation coefficient (R^2) was reported since this value is equal to the fraction of systematic variation between two variables.

3.4 Differential methylation

Differentially methylated loci were identified in three pairwise comparisons (LV versus RV, LV versus S, and RV versus S) using the *DML* function from the *SeSAME* package (Zhou et al. 2018) with the following input formula: (β ~ origin + id), where origin refers to the tissue section (LV, S or RV) and id refers to the tissue donor id. The output from the *DML* function was used to identify differentially methylated regions (DMR) using the *DMR* function from the *SeSAME* package (Zhou et al. 2018). In brief, the differentially methylated positions were combined in regions based on Euclidean distances. Next, a combined *p*-value was calculated using Stouffer's method (Stouffer et al. 1949). The resulting *p*-values were adjusted with the *p.adjust(method = "BH")* function in R. DMRs with a minimum of 5 CpGs and an adjusted *p*-value below 0.05 were considered significant and used for further analyses. The DMRs were annotated to nearby genes based on the *EPICv2.hg38.manifest.gencode.v41.tsv* manifest file (Kaur et al. 2023), available from https://zwdzwd.github.io/InfiniumAnnotation. Ensembl gene names were converted to gene names using the *getBM* function from the *biomaRt* R package (version 2.56.1) (Durinck et al. 2009).

3.5 Enrichment analysis

Gene ontology (GO) term overrepresentation analysis was conducted with the *clusterProfiler* R package (version 4.8.3). The *enrichGO* function was used to test the association between genes located in proximity to the DMRs and the two terms, "biological processes" and "molecular function". The *org.Hs.eg.db* (version 3.17.0) annotation package was used as the input database. Genes with one or more annotated DMRs were included in the background set as input for the *enrichGO* function. The *p*-values were adjusted with the default method (*pAdjustMethod = "BH"*) of the *enrichGO* function. Adjusted *p*-values below 0.05 were considered statistically significant. Overrepresentation analyses can be biased if a DMR is annotated to multiple nearby genes that share

the same gene ontology (GO) term. Therefore, we excluded a single gene ontology term (GO:0070003), which is driven only by a single DMR near two genes (*PSMB8* and *PSMB9*).

3.6 Postmortem computed tomography scans

Before the autopsy, the deceased individuals underwent a whole-body unenhanced computed tomography (CT) scan as part of the routine investigation. These postmortem CT scans were performed on a Siemens Somatom Definition 64 slice scanner (Siemens Healthcare, Erlangen, Germany) using a standard protocol with a tube voltage of 120 kV and automatic tube current modulation (reference mAs: 300 and effective mAs range: 240-300). Images of the thorax were reconstructed with 2.5 mm slice thickness using a standard soft tissue kernel. In one case, only the bone kernel reconstruction was available.

The LV and RV volumes (in cm^3) were estimated from the CT images that were assessed using Myrian Software (Intrasense, Montpellier, France), and the LV and RV volumes were calculated by manually contouring the RV and LV, using the "filled space" function of the region of interest (ROIs) on each axial slice, beginning from the demarcation of the ventricles from the atria to the apex. Each volume included the ventricular wall and the associated cavity, as it was not possible to separate them due to the lack of attenuation differences between the cavity and the surrounding ventricular muscle in the images. The epicardial fat was excluded. The interventricular septum was included in the LV volume. Image analysis was performed by a forensic pathologist with postmortem CT certification and more than 15 years of experience.

3.7 Ethics statement

Informed consent was obtained from relatives of the deceased individuals included in this study. Ventricular tissue was collected from the research biobank at the Section of Forensic Pathology, the Department of Forensic Medicine, University of Copenhagen (004-0064/21-7000 and 004-0022/18-7000). The project is registered at the University of Copenhagen's joint records of processing of personal data in research projects and biobanks (KU j.nr 514-0726/22-3000). The project complies with the rules of the General Data Protection Regulation (Regulation (EU) 2016/679). The study was approved by the Committees on Health Research Ethics in the Capital Region of Denmark (H18014656).

4 Results

4.1 DNA methylation of the ventricles of the human heart

Cardiac tissue was collected from 15 deceased individuals (13 males and two females) to investigate the DNA methylation patterns of the ventricles of the human heart (Figure 1A). The samples were collected from

individuals who died due to SCD. Tissue was collected from LV, S, and RV from the midventricular section. The boundaries of the age intervals ranged from 25-50 years (median 46 years).

In the first step of the analysis, the data were normalised and filtered to omit data from CpG sites with low-intensity signals. We only included data from CpG sites annotated to the autosomal chromosomes (chromosomes 1-22). After this step, data from 771,458 CpG sites remained. The 65 identification SNPs of the Infinium MethylationEPIC v2.0 array were used to exclude possible mislabelling of the paired samples from each individual (Fig. S1).

All samples showed the characteristic bimodal β-value distribution, which is expected for DNA methylation values from array analysis (Fig. S2). The squared Pearson's correlation coefficients (R^2) of the β-values ranged from 0.961 to 0.995 (median: 0.987) among all samples. In comparison, the median values of R^2 between LV, S, and RV of each individual ranged from 0.978 to 0.994 (median of medians: 0.991) (Fig. S3).

The overall variability of the data was investigated with a PCA of M-values (logit-transformed β-values). The first four components explained 33.1% of the total variation (Figure 1B). We observed no overall tendency for clustering based on the variability of all sites. Next, we investigated the variability among the 0.1% most variable positions corresponding to 771 positions (Figure 1C). The inter-individual variability of the samples exceeded the intra-individual variability in all samples except for those obtained from two individuals (ID #2 and #6), as shown by the dendrogram above the heatmap (Figure 1C), where RV deviated from LV and S in both individuals.

4.2 Differential methylation among the left and right ventricles, and the septum

The analysis of differential methylation was separated into three pairwise comparisons (LV vs RV, LV vs S, and RV vs S). A DMR refers to a specific genomic region where the DNA methylation levels are different in at least one of the pairwise comparisons (Figure 2A). In the three pairwise comparisons, 64 (LV-RV), 40 (LV-S), and 186 (RV-S) significant DMRs with 5 ≥ CpG positions were identified (Figure 2B and Table S1). However, since multiple DMRs were observed in two different pairwise comparisons, the total number of DMRs was 256, corresponding to the sum of the values within the Venn diagram.

The mean β-value differences of the DMRs ranged from -0.05 to 0.05 (LV-RV), from -0.046 to 0.062 (LV-S), and from -0.066 to 0.041 (RV-S) (Table S1). A positive mean β-value difference of the LV-RV comparison indicated that the DNA obtained from LV samples had higher methylation levels than samples from RV. In contrast, a negative value corresponded to a DMR with lower methylation levels in LV compared to RV. The majority of the 256 DMRs were detected in only one of the three pairwise comparisons (Figure 2B). However,

34 DMRs (corresponding to the sum of 23, 6, and 5 overlapping DMRs) were found in two of the three pairwise comparisons. In these cases, one tissue, e.g. LV, was differentially methylated relative to both S and RV, as illustrated in Fig. 2A. The median width among the 256 DMRs was 2,130 bp (interquartile range: 794-11,272 bp) and included information on DNA methylation levels of up to 30 CpG positions.

The DMRs were assigned to nearby genes (DMR-genes) to examine the potential biological role of the DMRs. Among the DMRs, 47 could not be assigned to any genes, while the remaining DMRs were assigned to between one and five genes. We conducted an overrepresentation analysis using the *clusterProfiler* R package (Wu et al. 2021). Overrepresentation analysis is a method that can be used to identify whether certain GO-terms of "*Biological Processes*" or "*Molecular Functions*" are more common among a set of genes than expected by chance.

The genes from the three comparisons (LV-S, LV-RV, and RV-S) were overrepresented among 46 biological processes after correction for multiple testing (Table S2), showing that these genes were observed more often than expected in each of these biological processes. Among the total of 46 overrepresented biological processes, 45 were observed for the LV-RV comparison (Figure 2C). The DMR genes of this comparison were overrepresented in terms such as "*cardiac chamber formation*", "*cardiac ventricle formation*", and "*positive regulation of heart growth*". Of these, the three most frequently involved genes were *MEF2C*, *NOTCH1*, and *TBX5* (Figure 2D). There were no overrepresented biological processes of the genes for the LV-S comparison. One biological process ("*cell morphogenesis involved in neuron differentiation*") was statistically significantly enriched for the RV-S comparison.

The DMR-genes were also overrepresented among seven molecular function terms for the LV-RV comparison and two terms for the RV-S comparison (Table S3). The overrepresented molecular functions included "*DNA-binding transcription activator activity*", *"transcription coregulator binding*", and "*transcription coactivator binding*".

4.3 Molecular signatures of *PITX2* associated with left-right sidedness

Two DMRs overlapped either "paired-like homeodomain transcription factor 2" (*PITX2*) or "*PITX2* adjacent noncoding RNA" (*PANCR*) (Figures 3A-B). The first DMR, hereafter labelled as the *PANCR* DMR, overlapped *PANCR* at position chr4:110,610,770-110,612,796 and was identified in the LV-RV as well as the LV-S comparison (Figure 3A, left panel, and Figure 3B). The other DMR, hereafter labelled as the *PITX2* DMR, was located at position chr4:110,615,611-110,618,136 overlapping the 3' untranslated region of *PITX2* and was only identified in the LV-S comparison (Figure 3A, right panel, and Figure 3B).

To examine the transcriptional regulatory role of these DMRs in relation to differences between the left and right sides of the human heart, we compared our findings to previously published single-nuclei chromatin accessibility data (Hocker et al. 2021) and transcribed regulatory elements (Deviatiiarov et al. 2023). Single-nuclei profiling of chromatin accessibility is a method for identification of active regulatory regions that control gene expression in specific cell types (Cusanovich et al. 2015). We observed no differentially accessible regions between LV and RV that overlapped the *PANCR* DMR and the *PITX2* DMR. However, two differentially accessible regions between left and right atria overlapped both the *PANCR* and *PITX2* DMRs, and four other differentially accessible regions overlapped either the *PANCR* or the *PITX2* DMR (Figure 3B). Notably, all six differentially accessible regions were specific for cardiomyocytes and were more accessible in the left than the right atrium.

Next, we investigated transcribed regulatory elements based on cap analysis of gene expression (CAGE) of samples from the left and right sides of human hearts (Deviatiiarov et al. 2023). Based on the CAGE data from the original study, 35 transcribed regulatory elements were expressed more on the left than the right side of the heart. Among these, one transcribed regulatory element was associated with *PITX2,* and two transcribed regulatory elements were associated with *PANCR,* thereby suggesting that an alternative start site was used (Figure 3C).

4.4 Correlation of *PITX2* locus differential methylation with left ventricle volume

Due to the previous observations of differential accessibility and transcriptional activity, combined with our observation of the *PANCR* and *PITX2* DMRs*,* we proceeded to compare the β-values of the DMRs with the volume of LV as measured from postmortem CT scans.

There were no available CT measurements from three of the individuals. In two cases, postmortem CT was not performed because the scanner was unavailable at the time of the autopsy (#10 and #11). A third case (#14) was excluded due to a large amount of right-sided intraventricular air.

As expected, the heart weight was positively correlated with the volume of LV and S obtained from the CT scans (Pearson's $R^2 = 0.94$, $P = 1.57\times10^{-7}$) (Fig. S4). To account for the expected correlation between LV volume and body size, we adjusted the LV volume for body surface area. We compared the measure to the median β-value difference for the LV-RV and LV-S comparisons of the *PANCR* DMR and the LV-S comparison of the *PITX2* DMR (Figure 4). There was no significant correlation for the LV-RV comparison ($P = 0.341$). However, the median β-value differences were negatively correlated with the LV volume for the *PANCR* DMR (Pearson's $R^2 = 0.51$, $P = 0.009$) and the *PITX2* DMR (Pearson's $R^2 = 0.54$, $P = 0.007$) in the LV-S comparison. In other words, reduced DNA methylation of LV compared to S was associated with large LV volumes.

5 Discussion

5.1 Standardised tissue collection for postmortem investigations

In multiple studies, DNA methylation alterations of the human heart have been linked to different cardiac diseases (Haas et al. 2013; Grunert et al. 2016; Meder et al. 2017; Pepin et al. 2019a, 2019b; Sutter et al. 2024; Chen et al. 2025). However, a significant challenge is the inability to consistently collect tissue from the same anatomical locations of the heart for both cases and controls. Therefore, we standardised cardiac tissue collection in forensic autopsies and identified significant differences between tissue sections from the human heart.

Consistent with a previous investigation of DNA methylation from LV and RV from two individuals (Schultz et al. 2015), we found that the global DNA methylation signatures of cardiac ventricle samples are more similar within individuals than among individuals (Figures 1B-C). Despite this similarity, we identified DMRs among LV, S, and RV and showed their association with critical processes such as development, growth, and formation of the human heart (Figures 2C-D). In addition, the DMRs are assigned to well-known disease-associated genes. For instance, *TBX5* and *NOTCH1* are considered definitive genes for congenital heart disease (Morton et al. 2022), while common variants assigned to *TBX5* and *PITX2* are associated with atrial fibrillation (Christophersen et al. 2017; Roselli et al. 2018, 2025). Therefore, to avoid spurious findings, it is essential to collect and examine samples from different parts of the heart in a standardised manner and only compare cardiac tissues from the same anatomical location for DNA methylation investigation of cardiac diseases.

5.2 Differential methylation of *PANCR* and *PITX2* associated with left-right asymmetry

PITX2 is well-known for its role in establishing left-right asymmetry during embryonic development (Yoshioka et al. 1998; Liu et al. 2001; Mommersteeg et al. 2007). Therefore, we comprehensively investigated the DMRs in proximity to *PITX2* and *PANCR* and showed that the DMRs overlapped with cardiomyocyte-specific differentially accessible regions between left and right atria and transcribed regulatory elements associated with left-right sidedness of the heart (Figures 3A-C). In line with this finding, it was previously shown that *PITX2* and *PANCR* are more highly expressed in the left than the right atrium (Gore-Panter et al. 2016; Cranley et al. 2024). While we are unable to demonstrate the causality of the alteration, we highlight that DNA methylation and chromatin accessibility near *PITX2* and *PANCR* are associated with differential transcriptional activity between the left and right sides of the heart.

PITX2 and *PANCR* are expressed considerably less in the adult ventricles than in adult left atria (Bayraktar et al. 2024; Cranley et al. 2024). By perturbations of DNA methyltransferases, it was previously shown that *PITX2* promoter methylation was associated with reduced *PITX2* gene expression in human induced pluripotent stem

cells (Madsen et al. 2020) and that murine *Pitx2* promoter methylation was associated with reduced Pitx2 protein levels (Chen et al. 2025). Since increased DNA methylation levels are associated with reduced gene expression and protein levels, it may seem surprising that we observe DMRs in adult ventricles where *PITX2* is typically expressed in barely detectable levels. However, nuclear *Pitx2* is induced in adult ventricles of mice after myocardial infarction (Tao et al. 2016). Thus, the observed DNA methylation alterations may be a response to undetected heart injury. Alternatively, the *PITX2* and *PANCR* DMRs may be a stable signature from the past. Less than 1% of cardiomyocytes are replaced in the adult human heart each year (Bergmann et al. 2015). Therefore, DNA replication-dependent removal of DNA methylation signatures by passive demethylation should be considerably lower in cardiac tissue than in tissues with a high turnover.

5.3 Left ventricle volume associated with differential methylation of *PANCR* and *PITX2*

Recently, it was shown in a genome-wide association study that genetic variants assigned to *PITX2* were associated with the BSA-adjusted volume of left atria (Pirruccello et al. 2024). The identified lead variant (rs2634073) was located at position chr4:110,744,627, more than 120kb away from the *PITX2* gene. Here, we demonstrated that DNA methylation differences between LV and S in both the *PITX2* and *PANCR* DMRs were associated with LV volume as measured by postmortem CT scanning (Fig. 4). In line with these two findings, it was previously shown that atrial-specific *Pitx2* reduction enlarged the size of atria and ventricles in a murine model (Chinchilla et al. 2011). Interestingly, during the embryological state, morphological alterations were detected in the atria, but not in the ventricles, suggesting that the ventricular alterations are likely secondary to the dysfunction of the atria.

5.4 Strengths and limitations of the study

While CT-based ventricular volumetry is an established method in living subjects (Goo and Park 2015), a similar standardised image acquisition is not possible in autopsy cases. Unlike in living patients, the use of contrast agents and the ability to perform imaging during specific phases of the cardiac cycle, such as end-diastole, are not feasible postmortem. Hence, varying degrees of blood pooling in the ventricles can be observed postmortem, and the use of non-enhanced postmortem CT further complicates the differentiation of anatomical structures due to the lack of contrast between tissues.

Almost half of the included cases exhibited mild decomposition at the time of autopsy, which poses a risk of cardiovascular gas accumulating within the heart chambers, potentially leading to overestimation of ventricular volumes (Jackowski et al. 2006). In one case (#2), a hemopericardium, i.e. the presence of blood in the pericardial sac, caused cardiac compression, resulting in reduced ventricular volumes. In another case (#9), a surgical implant in the thoracic wall caused imaging artefacts, which may have affected the measurements.

Image analysis was performed by a single reader without assessment of intra- or inter-observer variability. Therefore, some degree of subjectivity and variability in the manual contouring of the images must be anticipated. Despite these limitations, the estimated ventricular volumes showed, as expected, a strong correlation with heart weight.

We conducted, to our knowledge, the most comprehensive characterisation of DNA methylation in the human ventricles to date. However, we acknowledge the limitations of the unbalanced sex distribution of our study. Male individuals are overrepresented in forensic autopsies (Larsen and Lynnerup 2011) and among autopsied SCDs (Winkel et al. 2017), which is reflected in this study. In the data analysis, we filtered the DMRs for the number of CpG sites and significance levels corrected for multiple testing. However, we did not filter for effect size for two reasons. First, since the analysis was conducted on bulk tissue, we expected that a stringent effect size threshold would exclude DMRs only present in a single cell type, e.g. cardiomyocytes. Second, due to the heterogeneity of the cause of death among young individuals, we expected heterogeneous DNA methylation patterns at genomic regions associated with any underlying disease causing SCD. While this decision possibly resulted in DMRs driven by high effect sizes in only a subset of the individuals, we demonstrated that the function of the identified DMRs and nearby genes was primarily related to biological processes necessary for cardiac and muscle growth and development.

5.5 Conclusion

Our findings showed that DNA methylation alterations near *PITX2* and *PANCR* are associated with left-right heart asymmetry and left ventricle size. The study demonstrates the importance of collecting samples from multiple regions of the cardiac ventricles in DNA methylation investigations of the human heart.

6 Acknowledgements

We thank Anja Ladegaard Jørgensen for technical assistance with this work. We sincerely thank all the relatives for their consent to this study.

7 Sources of Funding

This work was supported by the Ellen and Aage Andersen Fund. SNNC was supported by a research grant from the Danish Cardiovascular Academy, which is funded by the Novo Nordisk Foundation, grant number NNF20SA0067242, and the Danish Heart Foundation.

8 Disclosures

All authors declare no conflicts of interest.

9 Author contributions

S.N.N.C., M.L.K., J.B., N.M., J.T.H., and J.D.A. designed the study. K.B., S.T.L., P.H.H., M.K.P., and J.B. conducted the autopsies and postmortem CT scans, collected the tissue, and obtained informed consent for the study from the relatives of the deceased individuals. S.B.J. and M.L.K. processed the samples and conducted the experiments. S.N.N.C., K.B., S.T.L., M.M.A., and J.D.A. performed the data analysis. S.N.N.C., K.B., S.T.L., J.T.H., and J.D.A. wrote the initial draft of the manuscript. All authors revised and approved the final manuscript.

10 Data availability

The data are available from the corresponding authors upon reasonable request.

11 Figures

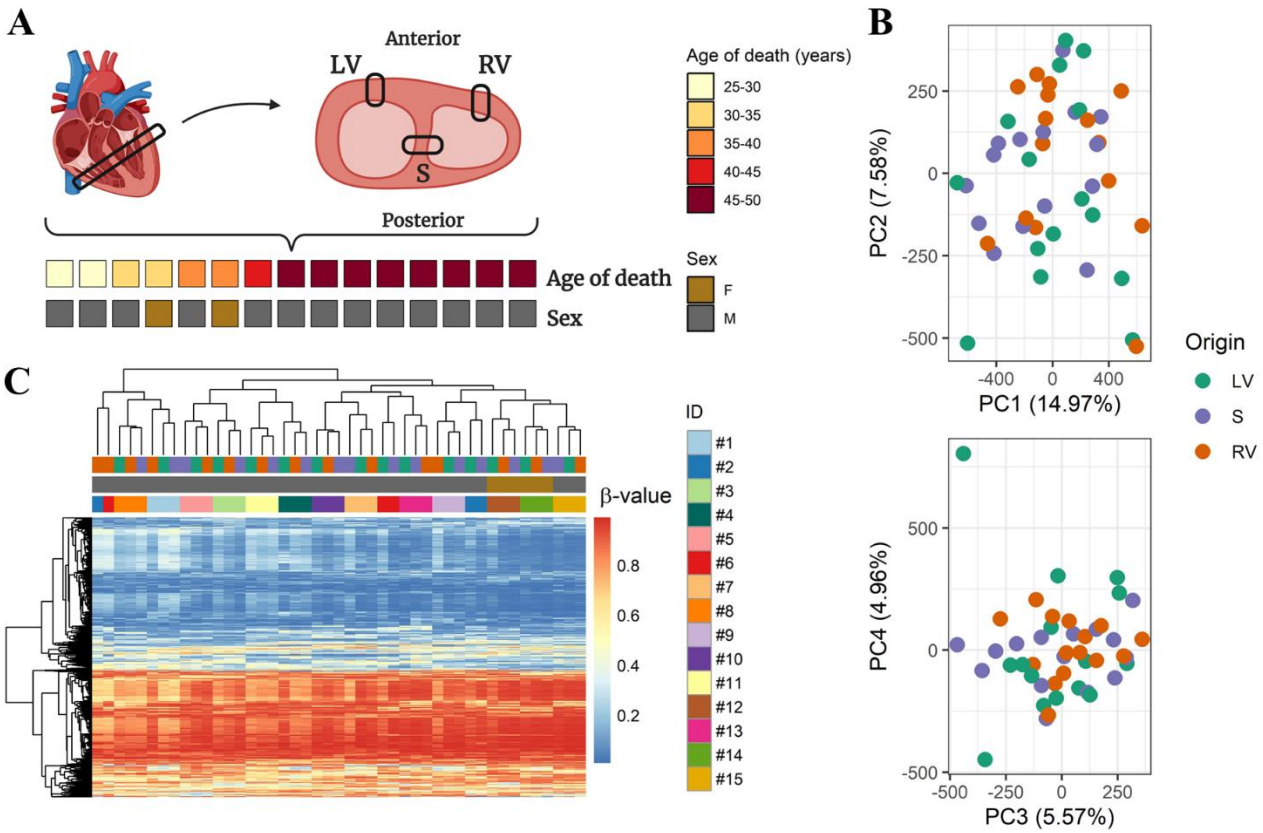

Figure 1. DNA methylation patterns of the ventricles of the heart. (A) Overview of the sampling procedure from the left ventricle (LV), septum (S), and the right ventricle (RV). The sex and age at death of the individuals. The age at death is visualised by colours in five-year intervals. (B) Principal component (PC) analysis of M-values from 771,458 positions coloured according to the origin of the tissue samples. (C) Heatmap of the 0.1 percentile of the positions (n = 771) with the highest variability among the samples. The colours below the dendrogram represent the origin of the samples and sex according to (A) and (B).

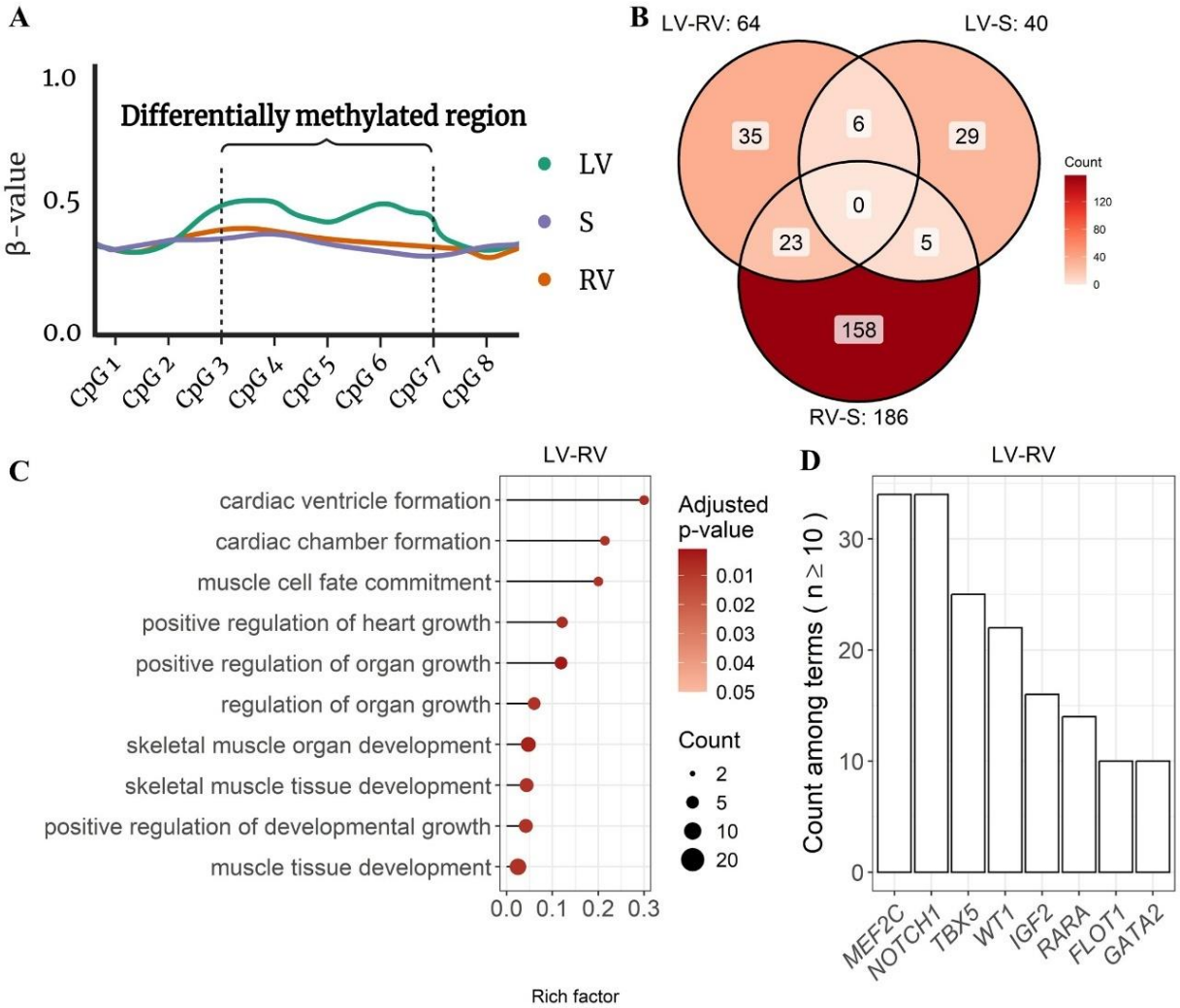

Figure 2. Differentially methylated regions of the ventricles. (A) Illustration of a differentially methylated region (DMR) with 5 CpG sites. The DMRs were investigated in three pairwise investigations among the left ventricle (LV), septum (S), and right ventricle (RV). In this illustration, the region was differentially methylated between LV and S and between LV and RV, illustrating the potential overlap among the identified DMRs in the three pairwise investigations. (B) Counts of differentially methylated regions (DMR) among the three pairwise comparisons (LV-RV, LV-S, and RV-S). (C) Gene ontology (GO) overrepresentation analysis of biological processes among the DMRs between LV and RV. The ten terms with the highest rich factor (ratio of DMR-genes divided by all genes in the specific term) are visualised. (D) Count of Gene Ontology terms that each gene is assigned to (genes associated with < 10 significant terms are not included in the figure).

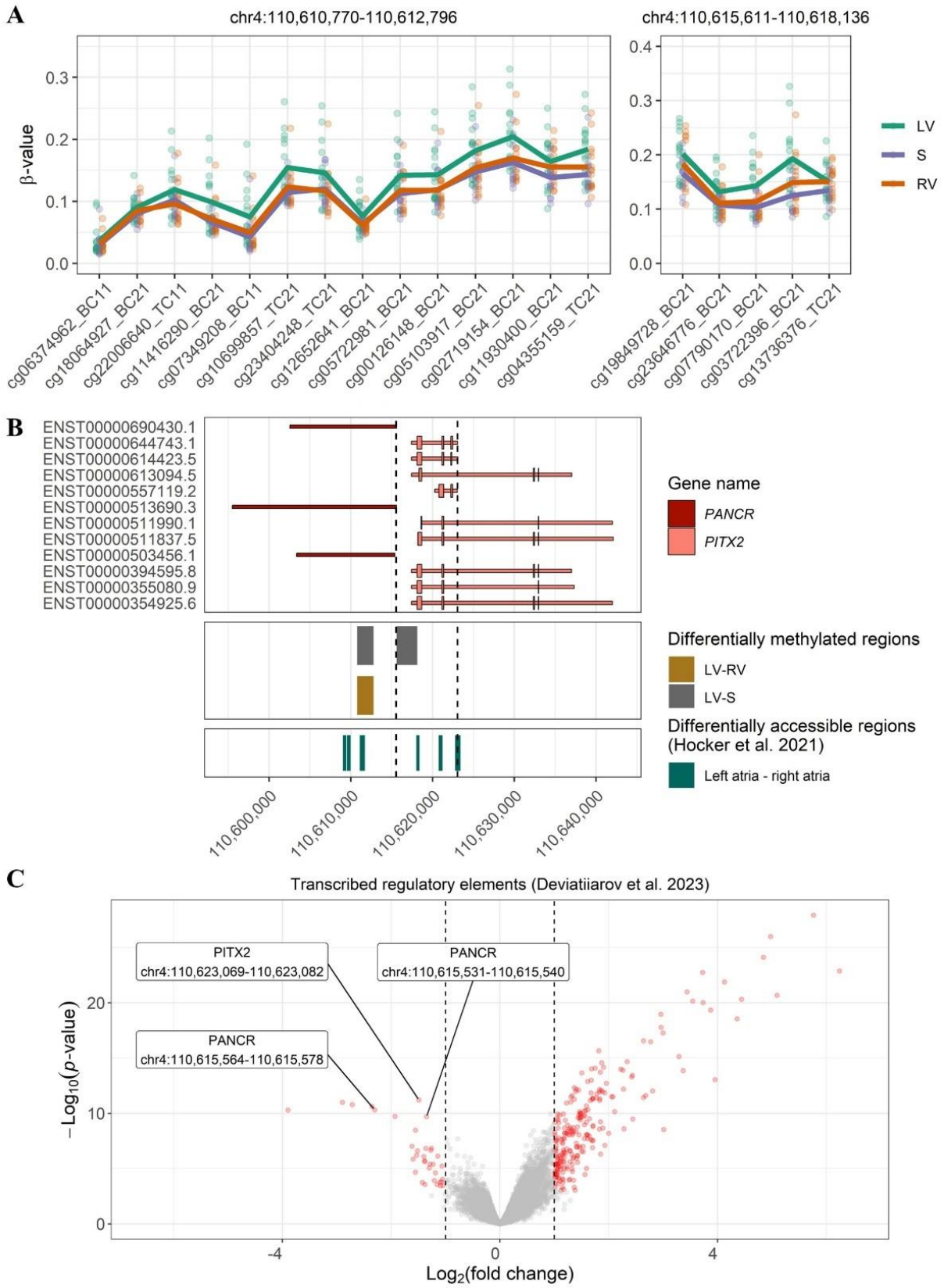
A
chr4:110,610,770-110,612,796
chr4:110,615,611-110,618,136
β-value
LV
S
RV
cg06374962_BC11
cg18064927_BC21
cg22006640_TC11
cg11416290_BC21
cg07349208_BC11
cg10699857_TC21
cg23404248_TC21
cg12652641_BC21
cg05722981_BC21
cg00126148_BC21
cg05103917_BC21
cg02719154_BC21
cg11930400_BC21
cg04355159_TC21
cg19849728_BC21
cg23646776_BC21
cg07790170_BC21
cg03722396_BC21
cg13736376_TC21
B
ENST00000690430.1
ENST00000644743.1
ENST00000614423.5
ENST00000613094.5
ENST00000557119.2
ENST00000513690.3
ENST00000511990.1
ENST00000511837.5
ENST00000503456.1
ENST00000394595.8
ENST00000355080.9
ENST00000354925.6
Gene name
PANCR
PITX2
Differentially methylated regions
LV-RV
LV-S
Differentially accessible regions
(Hocker et al. 2021)
Left atria - right atria
110,600,000
110,610,000
110,620,000
110,630,000
110,640,000
C
Transcribed regulatory elements (Deviatiiarov et al. 2023)
PITX2
chr4:110,623,069-110,623,082
PANCR
chr4:110,615,531-110,615,540
PANCR
chr4:110,615,564-110,615,578
−Log10(p-value)
Log2(fold change)

369

Figure 3. Differentially methylated regions at the *PANCR-PITX2* locus. (A) β-values per position are shown for two differentially methylated regions (DMRs) located in proximity to "paired-like homeodomain transcription factor 2" (*PITX2*) and "*PITX2* adjacent noncoding RNA" (*PANCR*). The mean β-values per position among each tissue are shown as lines covering the positions. Each value on the horizontal axis corresponds to the unique identifier of the positions with differential methylation. (B) Position and direction of transcription for *PANCR* and *PITX2*. The *PANCR* DMR (chr4:110,610,770-110,612,796) was differentially methylated in two comparisons (LV-RV and LV-S) while the *PITX2* DMR (chr4:110,615,611-110,618,136) was differentially methylated only in the comparison of LV-S. Both DMRs overlapped with previously identified differentially accessible regions between left and right atria (Hocker et al. 2021). (C) Volcano plot based on previous investigation of transcribed regulatory elements between the left and right side of the heart (Deviatiiarov et al. 2023). Negative fold change values correspond to the transcribed regulatory elements that are more active in the left than the right side of the heart. The locations of the three significant transcribed regulatory elements annotated to *PANCR* and *PITX2* correspond to the vertical dashed lines in B. LV: Left ventricle, S: septum, RV: right ventricle.

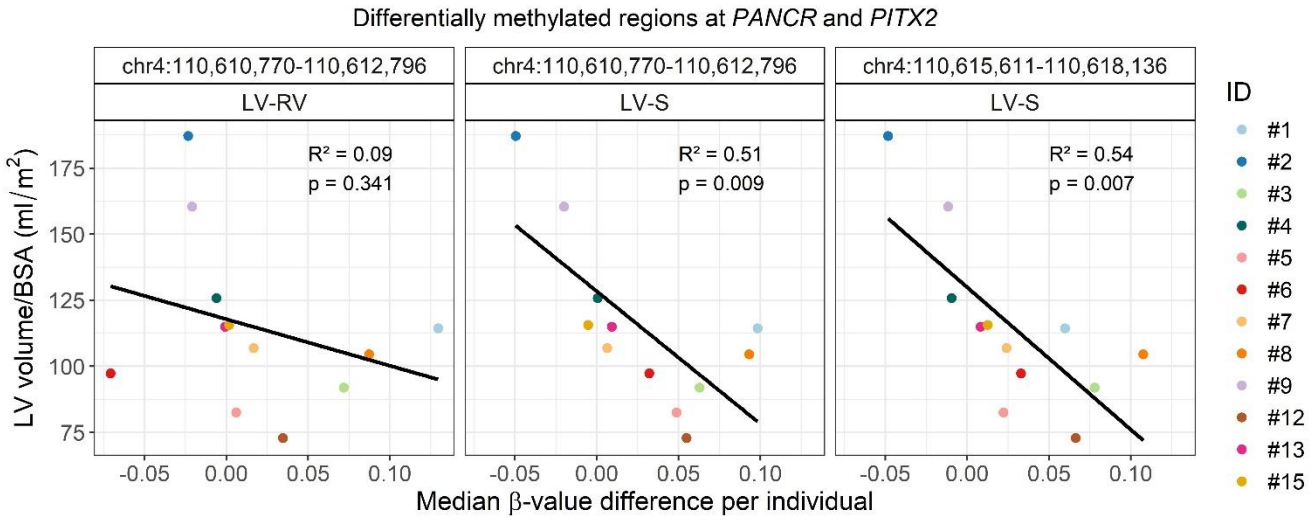

Figure 4. Association of *PANCR-PITX2* DNA methylation with left ventricular volume. Left ventricle volume corrected for body surface area (BSA) against the median β-value difference of each individual within the differentially methylated region assigned to *PANCR* and *PITX2*. Pearson's squared correlation coefficient (R^2) and *p*-values are shown in the upper right corner of the panels. The black lines indicate the regression lines based on a linear model.

References

Basso C, Aguilera B, Banner J, Cohle S, D'Amati G, Gouveia RH de, et al. Guidelines for autopsy investigation of sudden cardiac death: 2017 update from the Association for European Cardiovascular Pathology. Virchows Archiv. 2017;471(6):691–705.

Bayraktar S, Cranley J, Kanemaru K, Knight-Schrijver V, Colzani M, Davaapil H, et al. High-resolution atlas of the developing human heart and the great vessels. bioRxiv. 2024;2024.04.27.591127.

Bergmann O, Zdunek S, Felker A, Salehpour M, Alkass K, Bernard S, et al. Dynamics of Cell Generation and Turnover in the Human Heart. Cell. 2015;161(7):1566–75.

Chen Q, Zheng A, Xu X, Shi Z, Yang M, Sun S, et al. Nrf3-Mediated Mitochondrial Superoxide Promotes Cardiomyocyte Apoptosis and Impairs Cardiac Functions by Suppressing Pitx2. Circulation. 2025;

Chinchilla A, Daimi H, Lozano-Velasco E, Dominguez JN, Caballero R, Delpón E, et al. PITX2 Insufficiency Leads to Atrial Electrical and Structural Remodeling Linked to Arrhythmogenesis. Circ: Cardiovasc Genet. 2011;4(3):269–79.

Christiansen SN, Andersen JD, Kampmann ML, Liu J, Andersen MM, Tfelt-Hansen J, et al. Reproducibility of the Infinium methylationEPIC BeadChip assay using low DNA amounts. Epigenetics [Internet]. 2022;00(00):1–10. Available from: https://www.tandfonline.com/doi/full/10.1080/15592294.2022.2051861

Christophersen IE, Rienstra M, Roselli C, Yin X, Geelhoed B, Barnard J, et al. Large-scale analyses of common and rare variants identify 12 new loci associated with atrial fibrillation. Nature Genetics. 2017;49(6):946–52.

Cranley J, Kanemaru K, Bayraktar S, Knight-Schrijver V, Pett JP, Polanski K, et al. Multiomic analysis reveals developmental dynamics of the human heart in health and disease. bioRxiv. 2024;2024.04.29.591736.

Cusanovich DA, Daza R, Adey A, Pliner HA, Christiansen L, Gunderson KL, et al. Multiplex single-cell profiling of chromatin accessibility by combinatorial cellular indexing. Science. 2015;348(6237):910–4.

Deviatiiarov RM, Gams A, Kulakovskiy IV, Buyan A, Meshcheryakov G, Syunyaev R, et al. An atlas of transcribed human cardiac promoters and enhancers reveals an important role of regulatory elements in heart failure. Nat Cardiovasc Res. 2023;2(1):58–75.

Du P, Zhang X, Huang CC, Jafari N, Kibbe WA, Hou L, et al. Comparison of Beta-value and M-value methods for quantifying methylation levels by microarray analysis. BMC Bioinformatics. 2010;11.

Durinck S, Spellman PT, Birney E, Huber W. Mapping identifiers for the integration of genomic datasets with the R/Bioconductor package biomaRt. Nat Protoc. 2009;4(8):1184–91.

Gilsbach R, Schwaderer M, Preissl S, Grüning BA, Kranzhöfer D, Schneider P, et al. Distinct epigenetic programs regulate cardiac myocyte development and disease in the human heart in vivo. Nature Communications. 2018;9(1):391.

Goo HW, Park SH. Semiautomatic three-dimensional CT ventricular volumetry in patients with congenital heart disease: agreement between two methods with different user interaction. Int J Cardiovasc Imaging. 2015;31(Suppl 2):223–32.

Gore-Panter SR, Hsu J, Barnard J, Moravec CS, Wagoner DRV, Chung MK, et al. PANCR, the PITX2 Adjacent Noncoding RNA, Is Expressed in Human Left Atria and Regulates PITX2c Expression. Circulation: Arrhythmia and Electrophysiology. 2016;9(1).

Grunert M, Dorn C, Cui H, Dunkel I, Schulz K, Schoenhals S, et al. Comparative DNA methylation and gene expression analysis identifies novel genes for structural congenital heart diseases. Cardiovascular Research. 2016;112(1):464–77.

Haas J, Frese KS, Park YJ, Keller A, Vogel B, Lindroth AM, et al. Alterations in cardiac DNA methylation in human dilated cardiomyopathy. EMBO Mol Med. 2013;5(3):413–29.

Hocker JD, Poirion OB, Zhu F, Buchanan J, Zhang K, Chiou J, et al. Cardiac cell type-specific gene regulatory programs and disease risk association. Science Advances. 2021;7(20):1–24.

Jackowski C, Thali MJ, Buck U, Aghayev E, Sonnenschein M, Yen K, et al. Noninvasive Estimation of Organ Weights by Postmortem Magnetic Resonance Imaging and Multislice Computed Tomography. Investig Radiol. 2006;41(7):572–8.

Jean-Philippe E, Lerner I, Valentin E, Folke F, Böttiger B, Gislason G, et al. Incidence of Sudden Cardiac Death in the European Union. Journal of the American College of Cardiology. 2022;79(18):1818–27.

Kaur D, Lee SM, Goldberg D, Spix NJ, Hinoue T, Li HT, et al. Comprehensive evaluation of the Infinium human MethylationEPIC v2 BeadChip. Epigenetics Communications 2023 3:1 [Internet]. 2023;3(1):1–15. Available from: https://epicom.biomedcentral.com/articles/10.1186/s43682-023-00021-5 http://creativecom-mons.org/publicdomain/zero/1.0/

Lahrouchi N, Raju H, Lodder EM, Papatheodorou E, Ware JS, Papadakis M, et al. Utility of Post-Mortem Genetic Testing in Cases of Sudden Arrhythmic Death Syndrome. Journal of the American College of Cardiology. 2017;69(17):2134–45.

Lahrouchi N, Raju H, Lodder EM, Papatheodorou S, Miles C, Ware JS, et al. The yield of postmortem genetic testing in sudden death cases with structural findings at autopsy. European Journal of Human Genetics. 2020;28(1):17–22.

Larsen ST, Lynnerup N. Medico-legal autopsies in Denmark. Dan Méd Bull. 2011;58(3):A4247.

Leek JT, Johnson WE, Parker HS, Jaffe AE, Storey JD. The sva package for removing batch effects and other unwanted variation in high-throughput experiments. Bioinformatics. 2012;28(6):882–3.

Liu C, Liu W, Lu MF, Brown NA, Martin JF. Regulation of left-right asymmetry by thresholds of Pitx2c activity. Development. 2001;128(11):2039–48.

Lynge TH, Nielsen JL, Risgaard B, Werf C van der, Winkel BG, Tfelt-Hansen J. Causes of sudden cardiac death according to age and sex in persons aged 1–49 years. Heart Rhythm [Internet]. 2022;20(1):61–8. Available from: https://doi.org/10.1016/j.hrthm.2022.08.036

Madsen A, Höppner G, Krause J, Hirt MN, Laufer SD, Schweizer M, et al. An Important Role for DNMT3A-Mediated DNA Methylation in Cardiomyocyte Metabolism and Contractility. Circulation [Internet]. 2020;142(16):1562–78. Available from: https://www.ahajournals.org/doi/10.1161/CIRCULATIONAHA.119.044444

Meder B, Haas J, Sedaghat-Hamedani F, Kayvanpour E, Frese K, Lai A, et al. Epigenome-Wide Association Study Identifies Cardiac Gene Patterning and a Novel Class of Biomarkers for Heart Failure. Circulation [Internet]. 2017;136(16):1528–44. Available from: https://www.ahajournals.org/doi/10.1161/CIRCULATIONAHA.117.027355

Mommersteeg MTM, Hoogaars WMH, Prall OWJ, Vries C de G de, Wiese C, Clout DEW, et al. Molecular Pathway for the Localized Formation of the Sinoatrial Node. Circ Res. 2007;100(3):354–62.

Morton SU, Quiat D, Seidman JG, Seidman CE. Genomic frontiers in congenital heart disease. Nat Rev Cardiol. 2022;19(1):26–42.

Pedersen TL. patchwork: The Composer of Plots [Internet]. 2024. Available from: https://patchwork.data-imaginist.com

Pepin ME, Drakos S, Ha CM, Tristani-Firouzi M, Selzman CH, Fang JC, et al. DNA methylation reprograms cardiac metabolic gene expression in end-stage human heart failure. American Journal of Physiology-Heart and Circulatory Physiology [Internet]. 2019a;317(4):H674–84. Available from: https://www.physiology.org/doi/10.1152/ajpheart.00016.2019

Pepin ME, Ha CM, Crossman DK, Litovsky SH, Varambally S, Barchue JP, et al. Genome-wide DNA methylation encodes cardiac transcriptional reprogramming in human ischemic heart failure. Laboratory Investigation [Internet]. 2019b;99(3):371–86. Available from: http://dx.doi.org/10.1038/s41374-018-0104-x

Pirruccello JP, Achille PD, Choi SH, Rämö JT, Khurshid S, Nekoui M, et al. Deep learning of left atrial structure and function provides link to atrial fibrillation risk. Nat Commun. 2024;15(1):4304.

Poggiali B, Dupont ME, Jacobsen SB, Smerup MH, Christiansen SNN, Tfelt-Hansen J, et al. DNA methylation stability in cardiac tissues kept at different temperatures and time intervals. Sci Rep. 2024;14(1):25170.

Roselli C, Chaffin MD, Weng LC, Aeschbacher S, Ahlberg G, Albert CM, et al. Multi-ethnic genome-wide association study for atrial fibrillation. Nature Genetics. 2018;50(9):1225–33.

Roselli C, Surakka I, Olesen MS, Sveinbjornsson G, Marston NA, Choi SH, et al. Meta-analysis of genome-wide associations and polygenic risk prediction for atrial fibrillation in more than 180,000 cases. Nat Genet. 2025;1–9.

Schultz MD, He Y, Whitaker JW, Hariharan M, Mukamel EA, Leung D, et al. Human body epigenome maps reveal noncanonical DNA methylation variation. Nature. 2015;523(7559):212–6.

Skjelbred T, Warming PE, Krøll J, Andersen MP, Torp-Pedersen C, Winkel BG, et al. Sudden Cardiac Death as First Manifestation of Cardiovascular Disease A Nationwide Study of 54,028 Deaths. JACC: Clin Electrophysiol. 2025;11(5):881–90.

Stiles MK, Wilde AAM, Abrams DJ, Ackerman MJ, Albert CM, Behr ER, et al. 2020 APHRS/HRS expert consensus statement on the investigation of decedents with sudden unexplained death and patients with sudden cardiac arrest, and of their families. Heart Rhythm [Internet]. 2021;18(1):e1–50. Available from: https://linkinghub.elsevier.com/retrieve/pii/S154752712030953X

Stouffer SA, Suchman EA, Devinney LC, Star SA, Jr. RMW. The American soldier: Adjustment during army life. (Studies in social psychology in World War II), Vol. 1. The American soldier: Adjustment during army life (Studies in social psychology in World War II), Vol 1. 1949;xii, 599–xii, 599.

Sutter C, Haas C, Bode PK, Neubauer J, Andersen JD. Exploratory DNA methylation analysis in post-mortem heart tissue of sudden unexplained death. Clin Epigenetics. 2024;16(1):167.

Tao G, Kahr PC, Morikawa Y, Zhang M, Rahmani M, Heallen TR, et al. Pitx2 promotes heart repair by activating the antioxidant response after cardiac injury. Nature. 2016;534(7605):119–23.

Wickham H. Journal of Statistical Software Tidy Data. 2014;59(10).

Wickham H, Averick M, Bryan J, Chang W, McGowan L, François R, et al. Welcome to the Tidyverse. Journal of Open Source Software. 2019;4(43):1686.

Wilde AAM, Semsarian C, Márquez MF, Shamloo AS, Ackerman MJ, Ashley EA, et al. European Heart Rhythm Association (EHRA)/Heart Rhythm Society (HRS)/Asia Pacific Heart Rhythm Society (APHRS)/Latin American Heart Rhythm Society (LAHRS) Expert Consensus Statement on the state of genetic testing for cardiac diseases. EP Europace. 2022;1–61.

Winkel BG, Risgaard B, Bjune T, Jabbari R, Lynge TH, Glinge C, et al. Gender differences in sudden cardiac death in the young-a nationwide study. BMC Cardiovascular Disorders. 2017;17(1):19.

Wu T, Hu E, Xu S, Chen M, Guo P, Dai Z, et al. clusterProfiler 4.0: A universal enrichment tool for interpreting omics data. Innov. 2021;2(3):100141.

Yoshioka H, Meno C, Koshiba K, Sugihara M, Itoh H, Ishimaru Y, et al. Pitx2, a Bicoid-Type Homeobox Gene, Is Involved in a Lefty-Signaling Pathway in Determination of Left-Right Asymmetry. Cell. 1998;94(3):299–305.

Zeppenfeld K, Tfelt-Hansen J, Riva M de, Winkel BG, Behr ER, Blom NA, et al. 2022 ESC Guidelines for the management of patients with ventricular arrhythmias and the prevention of sudden cardiac death. European heart journal [Internet]. 2022;43(40):3997–4126. Available from: https://academic.oup.com/eurheartj/advance-article/doi/10.1093/eurheartj/ehac262/6675633 https://academic.oup.com/eurheartj/article/43/40/3997/6675633 http://www.ncbi.nlm.nih.gov/pubmed/36017572

Zhou W, Triche TJ, Laird PW, Shen H. SeSAMe: Reducing artifactual detection of DNA methylation by Infinium BeadChips in genomic deletions. Nucleic Acids Research. 2018;46(20):1–15.